

Supplementary Materials for

Metabolic determinants of cellular fitness dependent on mitochondrial reactive oxygen species

Hyewon Kong, Colleen R. Reczek, Gregory S. McElroy, Elizabeth M. Steinert, Tim Wang,
David M. Sabatini, Navdeep S. Chandel*

*Corresponding author. Email: nav@northwestern.edu

Published 4 November 2020, *Sci. Adv.* **6**, eabb7272 (2020)
DOI: [10.1126/sciadv.abb7272](https://doi.org/10.1126/sciadv.abb7272)

This PDF file includes:

Figs. S1 to S9
Table S1

Supplementary Materials

Figure S1.

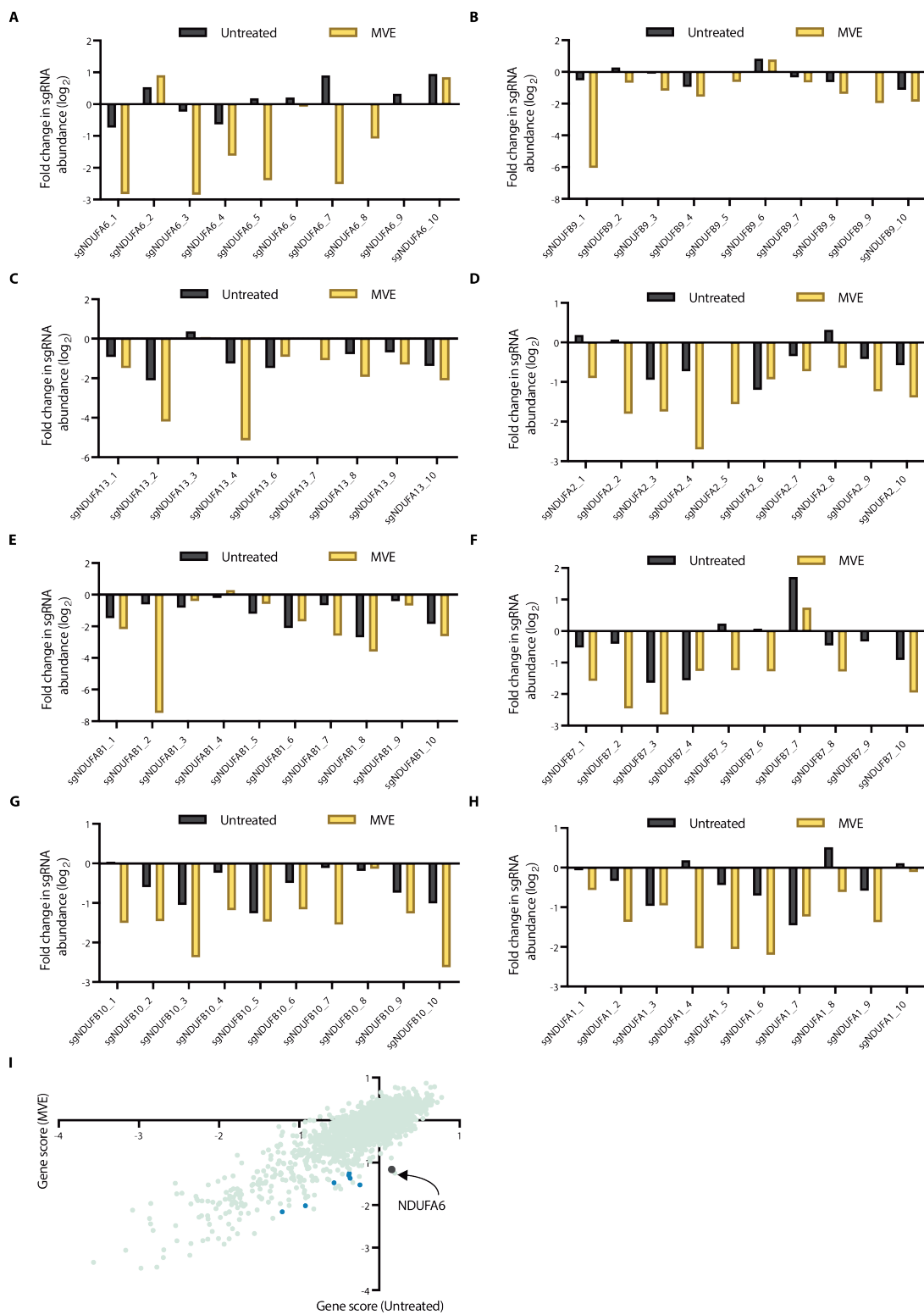


Fig. S1. A CRISPR-based negative selection screen identifies multiple subunits of mitochondrial complex I to be essential for cellular fitness in the presence of MVE.

(A-H) Changes in the abundance of individual sgRNAs targeting mitochondrial complex I subunit genes; *NDUFA6* (A), *NDUFB9* (B), *NDUFA13* (C), *NDUFA2* (D), *NDUFAB1* (E), *NDUFB7* (F), *NDUFB10* (G), and *NDUFA1* (H), in the presence (yellow) or absence (grey) of MVE. **(I)** Gene scores of all genes targeted by the metabolic sgRNA library in untreated (X-axis) versus MVE-treated (Y-axis) cell populations. Mitochondrial complex I subunit hits, *NDUFA6*, *NDUFB9*, *NDUFA13*, *NDUFA2*, *NDUFAB1*, *NDUFB7*, *NDUFB10*, and *NDUFA1*, are highlighted in blue. Among them, *NDUFA6*, indicated with an arrow, exhibited the largest differential gene score.

Figure S2.

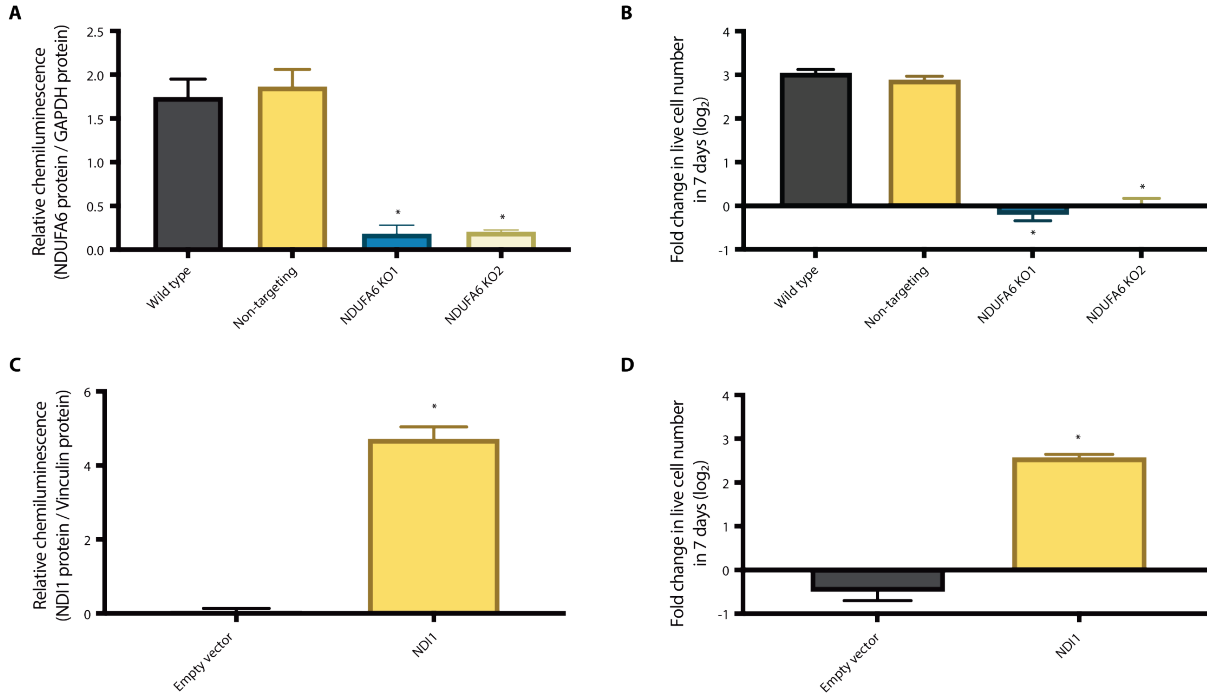


Fig. S2. CRISPR-mediated deletion of the *NDUFA6* gene impairs mitochondrial complex I function.

(A) Simple Western analysis of NDUFA6 protein in wild type, non-targeting control, and two NDUFA6-null (NDUFA6 KO1 and KO2) Jurkat cell lines. GAPDH was used as a loading control. (n=3, mean+s.e.m., *P=0.0003 compared to non-targeting) (B) Wild type, non-targeting control, and two NDUFA6-null (NDUFA6 KO1 and KO2) Jurkat cell lines were cultured in galactose media for 7 days, and the population doublings were assessed. (n=4, mean+s.e.m., *P<0.0001 compared to non-targeting) (C) Simple Western analysis of NDI1 protein expression in the NDUFA6 KO1 cell line with ectopic expression of either the empty vector or NDI1. Vinculin was used as a loading control. (n=3, mean+s.e.m., *P=0.0002 compared to empty vector) (D) NDUFA6 KO1 Jurkat cells expressing either empty vector or NDI1 were cultured in galactose media for 7 days, and the population doublings were assessed. (n=4, mean+s.e.m., *P<0.0001 compared to empty vector)

Figure S3.

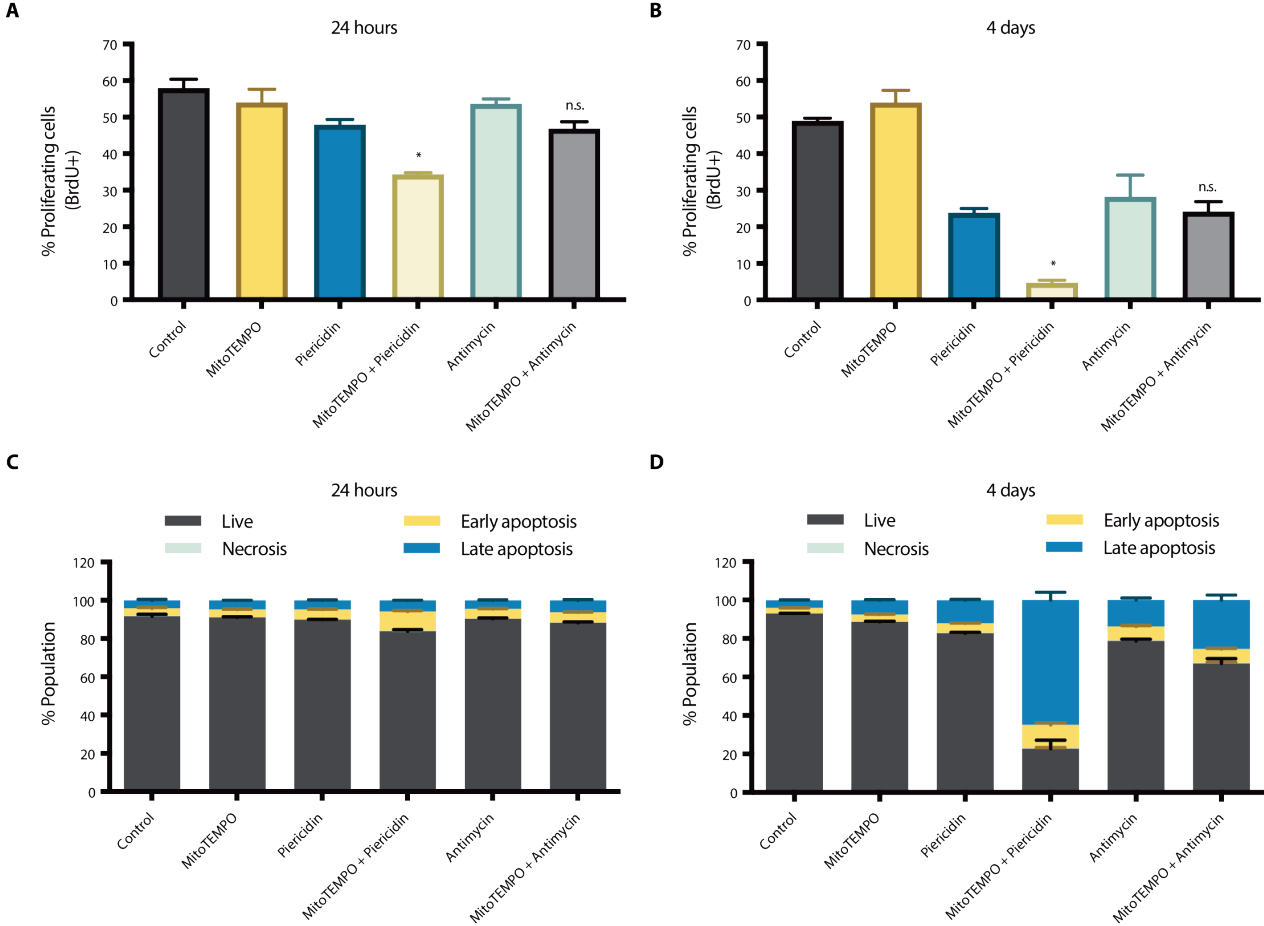


Fig. S3. Inhibition of mitochondrial complex I, but not mitochondrial complex III, synergizes with a mito-antioxidant to impair cellular fitness.

(A-B) Jurkat cells supplemented with pyruvate and uridine were treated with 1 μ M Piericidin or 1 μ M Antimycin +/- 400 μ M MitoTEMPO for 24 hours (A) or 4 days (B), and the percentage of BrdU incorporation into the proliferating cell population was measured. (n=3, mean+s.e.m., *P= 0.0093 (A) or *P= 0.0114 (B) compared to Piericidin alone, ^{n.s.}P=0.6588 (A) or ^{n.s.}P>0.9999 (B) compared to Antimycin alone) (C-D) Jurkat cells supplemented with pyruvate and uridine were treated with 1 μ M Piericidin or 1 μ M Antimycin +/- 400 μ M MitoTEMPO for 24 hours (C) or 4 days (D), and the percentage of Annexin V- and/or propidium iodine (PI)-incorporated apoptotic cell populations were measured. Live: Annexin V negative and PI negative; Necrosis: Annexin V negative and PI positive; Early apoptosis: Annexin V positive and PI negative; Late apoptosis: Annexin V positive and PI positive. (n=4, mean+s.e.m.)

Figure S4.

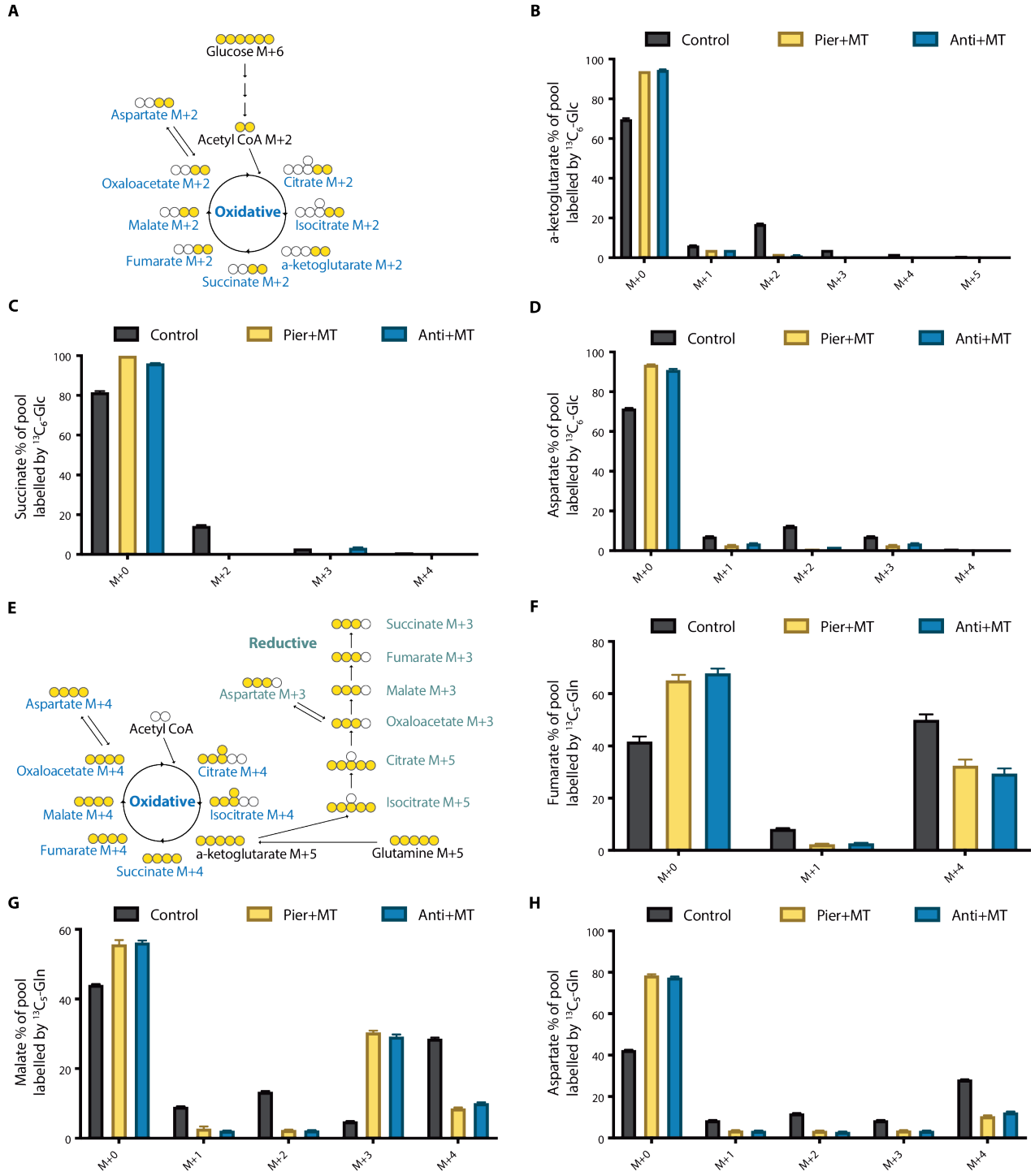


Fig. S4. Inhibition of mitochondrial complex I or mitochondrial complex III in the presence of a mito-antioxidant induces reductive TCA cycle.

(A) Schematic representation of the glucose-driven oxidative TCA cycle. Labelled carbons (^{13}C) are indicated in yellow. Oxidative TCA cycle of $[\text{U-}^{13}\text{C}_6]$ glucose results in M+2 pools of TCA-cycle metabolites, as well as aspartate. (B-D) Jurkat cells treated with vehicle (Control), Piericidin and MitoTEMPO (Pier+MT), or Antimycin and MitoTEMPO (Anti+MT) for 24 hours were labelled for 8 hours with $[\text{U-}^{13}\text{C}_6]$ glucose, and the percentages of labelled α -ketoglutarate (B), succinate (C), and aspartate (D) pools were assessed. (n=5, mean+s.e.m.) (C) Schematic representation of the glutamine-driven oxidative (blue) and reductive (green) TCA cycles. Labelled carbons (^{13}C) are indicated in yellow. Metabolism of $[\text{U-}^{13}\text{C}_5]$ glutamine results in fully labeled M+5 α -ketoglutarate. Oxidative TCA cycle of M+5 α -ketoglutarate generates M+4 pools of TCA-cycle metabolites, as well as aspartate. Reductive TCA cycle of M+5 α -ketoglutarate produces M+5 pool of (iso)citrate, followed by M+3 pool of malate. (F-H) Jurkat cells treated with vehicle (Control), Pier+MT, or Anti+MT for 24 hours were labelled for 8 hours with $[\text{U-}^{13}\text{C}_5]$ glutamine, and the percentages of labelled fumarate (F), malate (G), and aspartate (H) pools were assessed. (n=5, mean+s.e.m.)

Figure S5.

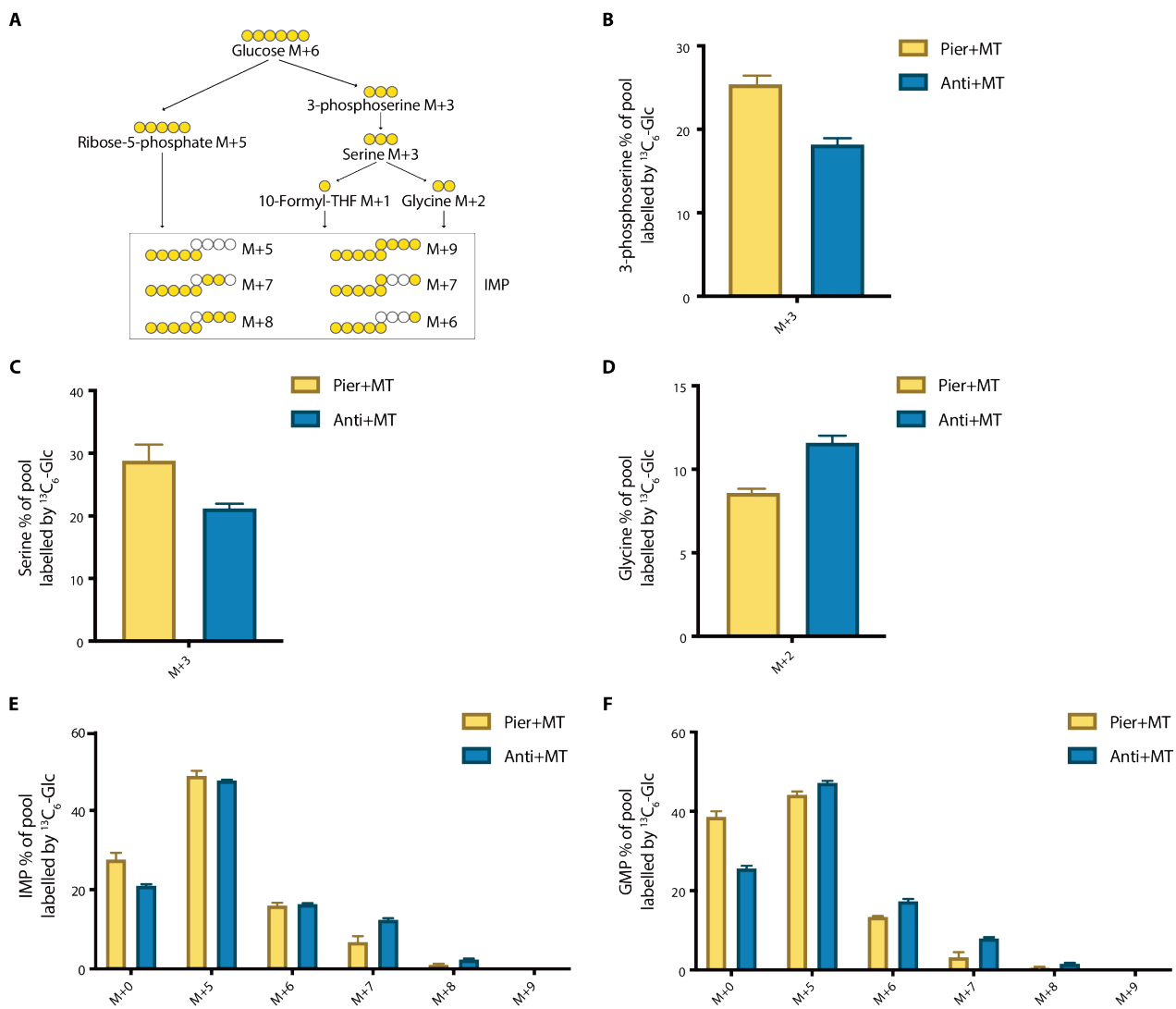


Fig. S5. Inhibition of mitochondrial complex I in the presence of a mito-antioxidant dysregulates one carbon metabolism and purine biosynthesis.

(A) Schematic representation of the glucose-driven one carbon metabolism and purine biosynthesis. Labelled carbons (^{13}C) are indicated in yellow. Metabolism of $[\text{U-}^{13}\text{C}_6]\text{glucose}$ generates M+3 pools of 3-phosphoserine and serine, followed by M+2 pool of glycine. M+2 glycine, when metabolized with fully labelled M+5 ribose-5-phosphate, can produce M+7 pool of purine precursor, IMP. (B-F) Jurkat cells treated with Piericidin and MitoTEMPO (Pier+MT), or Antimycin and MitoTEMPO (Anti+MT) for 24 hours were labelled for 8 hours with $[\text{U-}^{13}\text{C}_6]\text{glucose}$. The percentages of M+3 3-phosphoserine (B), M+3 serine (C), and M+2 glycine (D), labelled by glucose-driven one carbon metabolism were examined. Additionally, the percentages of labelled IMP purine precursor (E) and GMP purine (F) pools were assessed. (n=5, mean+s.e.m.).

Figure S6.

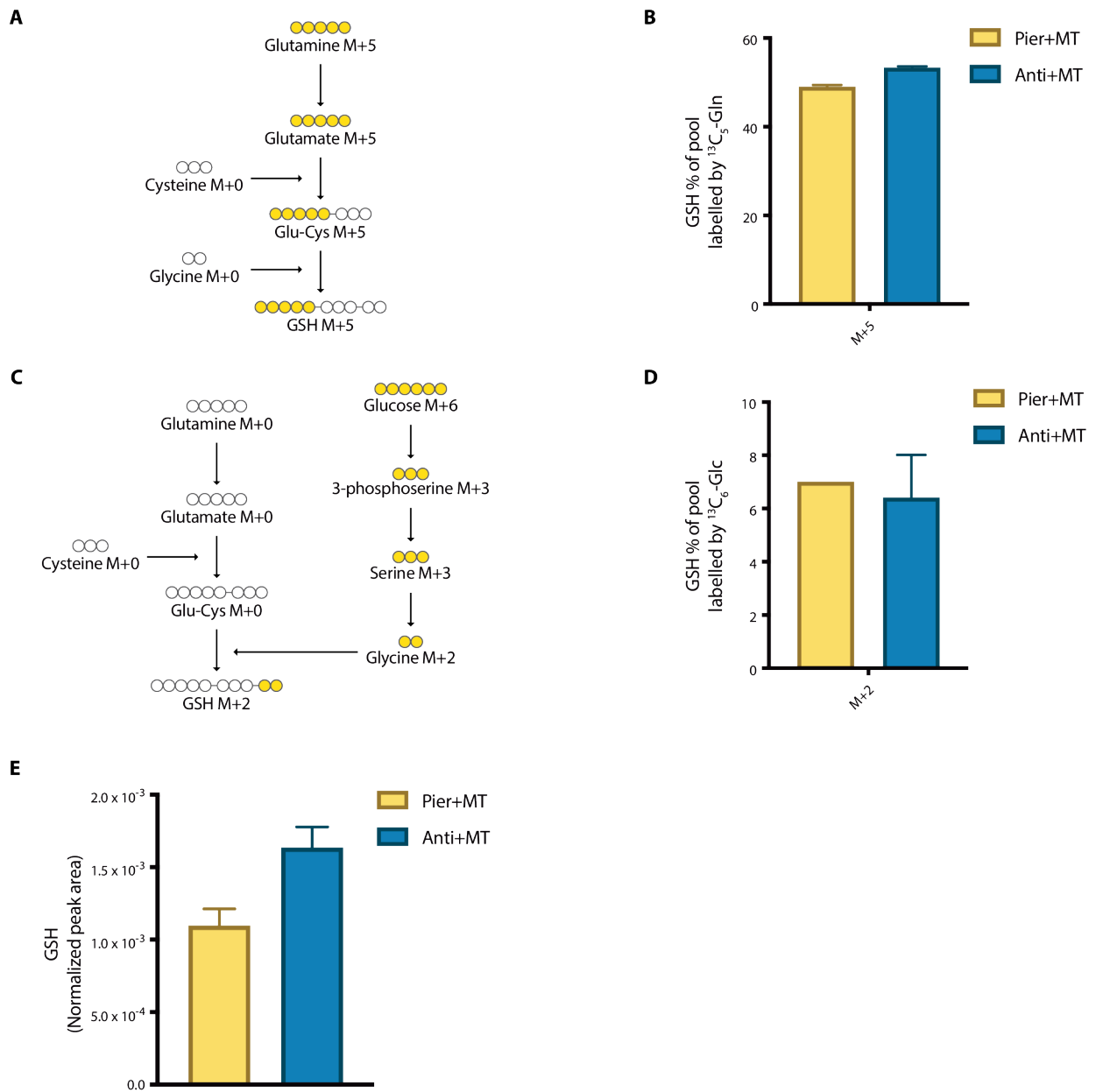


Fig. S6. Glutathione (GSH) content and synthesis in cells treated with Piericidin or Antimycin in combination with MitoTEMPO.

(A) Schematic representation of the glutamine-derived GSH synthesis. Labelled carbons (^{13}C) are indicated in yellow. Metabolism of $[\text{U-}^{13}\text{C}_5]\text{glutamine}$ results in M+5 pool of GSH. (B) Jurkat cells treated with Piericidin and MitoTEMPO (Pier+MT), or Antimycin and MitoTEMPO (Anti+MT) for 24 hours were labelled for 8 hours with $[\text{U-}^{13}\text{C}_5]\text{glutamine}$, and the percentage of M+5 labelled GSH was assessed. (n=5, mean+s.e.m.) (C) Schematic representation of the glucose-derived GSH synthesis. Labelled carbons (^{13}C) are indicated in yellow. Metabolism of $[\text{U-}^{13}\text{C}_6]\text{glucose}$ results in M+2 pool of GSH. (D) Jurkat cells treated with Pier+MT or Anti+MT for 24 hours were labelled for 8 hours with $[\text{U-}^{13}\text{C}_6]\text{glucose}$, and the percentage of M+2 labelled GSH was assessed. (n=5, mean+s.e.m.) (E) GSH levels in Jurkat cells treated with Pier+MT or Anti+MT for 24 hours. (n=6, mean+s.e.m.)

Figure S7.

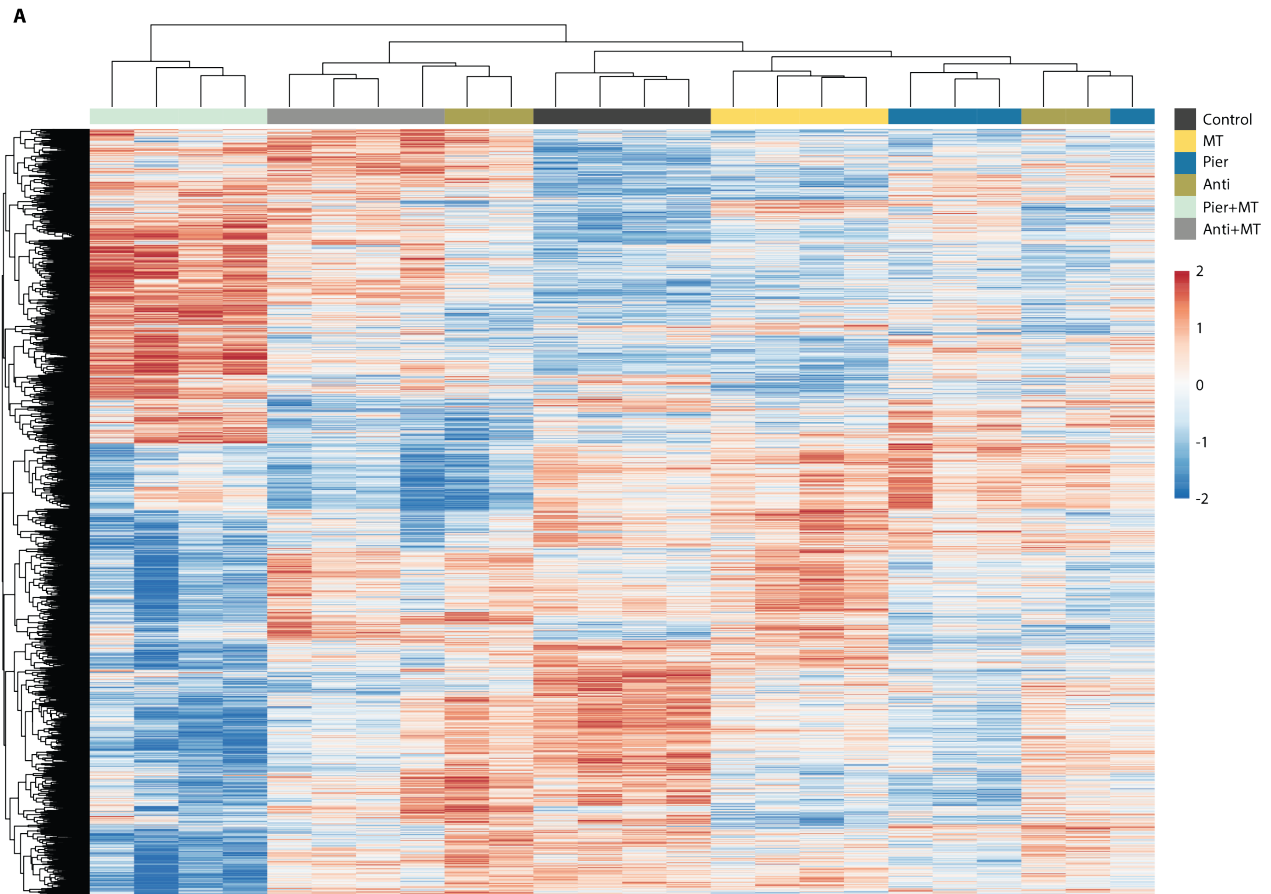


Fig. S7. Combination of mitochondrial complex I inhibition and a mito-antioxidant induces a unique transcriptomic signature.

(A) Heatmap of unsupervised clustering, representing RNA transcripts whose abundances were significantly different among Jurkat cells treated with vehicle (Control), MitoTEMPO (MT), Piericidin (Pier), Antimycin (Anti), Piericidin and MitoTEMPO (Pier+MT), or Antimycin and MitoTEMPO (Anti+MT) for 24 hours. The relative abundance of each transcript is depicted as z-score across rows. (Red: high; Blue: low) (n=4, FDR \leq 0.05)

Figure S8.

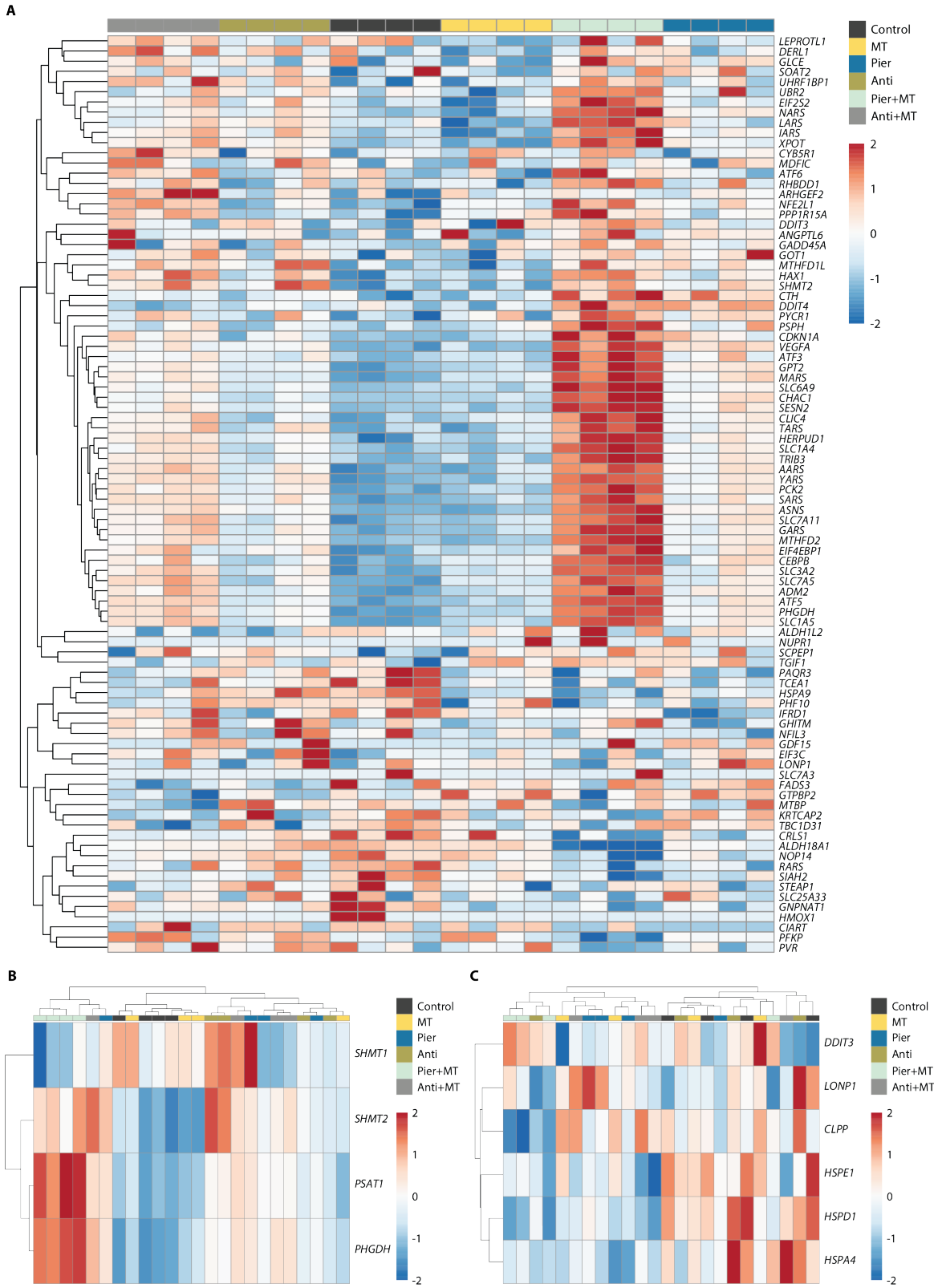


Fig. S8. ISR-associated genes are largely upregulated in Jurkat cells treated with Piericidin and MitoTEMPO.

(A) Heatmap of all ISR signature genes in Jurkat cells treated with vehicle (Control), MitoTempo (MT), Piericidin (Pier), Antimycin (Anti), Piericidin and MitoTEMPO (Pier+MT), or Antimycin and MitoTEMPO (Anti+MT) for 24 hours. The relative abundance of each transcript is depicted as z-score across rows. (Red: high; Blue: low) (n=4) (B-C) Heatmap of unsupervised clustering, representing one carbon metabolism (B) or canonical mitochondrial UPR (UPR^{mt}) (C) associated genes in Jurkat cells treated with vehicle (Control), MT, Pier, Anti, Pier+MT, or Anti+MT for 24 hours. The relative abundance of each transcript is depicted as z-score across rows. (Red: high; Blue: low) (n=4)

Fig. S9. Combination of mitochondrial complex I inhibition and a mito-antioxidant diminishes percentage of leukemic cells *in vivo*.

(A) Weight of spleens from T-ALL recipients treated with vehicle (Control), Phenformin, MitoTEMPO, or Phenformin+MitoTempo for 15 days. (Control: n=11; Phenformin: n=12; MitoTEMPO: n=12; Phenformin+MitoTEMPO: n=13., mean±s.e.m., *P=0.0307 (Phenformin) or *P<0.0001 (Phenformin+MitoTEMPO) compared to control, ^{n.s.}P value is reported in the material and methods) **(B, C, D)** Percentage of GFP+ T-ALL cells in the spleen (B), bone marrow (C), or peripheral lymph nodes (D) from T-ALL recipients treated with vehicle (Control), Phenformin, MitoTEMPO, or Phenformin+MitoTempo for 15 days. (Control: n=11; Phenformin: n=12; MitoTEMPO: n=12; Phenformin+MitoTEMPO: n=13., mean±s.e.m., *P=0.0195 (B); *P=0.0382 (C; Phenformin); *P<0.0001 (C; Phenformin+MitoTEMPO); *P<0.0001 (D) compared to control, ^{n.s.}P values are reported in the material and methods)

Table S1. Human integrated stress response (ISR) associated genes

group	gene_id	symbol
gene.clic	ENSG00000090861	AARS
gene.clic	ENSG00000128165	ADM2
gene.clic	ENSG00000059573	ALDH18A1
gene.clic	ENSG00000136010	ALDH1L2
gene.clic	ENSG00000130812	ANGPTL6
gene.clic	ENSG00000116584	ARHGEF2
gene.clic	ENSG00000070669	ASNS
gene.clic	ENSG00000162772	ATF3
gene.clic	ENSG00000169136	ATF5
gene.clic	ENSG00000118217	ATF6
gene.clic	ENSG00000124762	CDKN1A
gene.clic	ENSG00000172216	CEBPB
gene.clic	ENSG00000128965	CHAC1
gene.clic	ENSG00000159208	CIART
gene.clic	ENSG00000169504	CLIC4
gene.clic	ENSG00000182372	CLN8
gene.clic	ENSG00000088766	CRLS1

gene.clic	ENSG00000116761	CTH
gene.clic	ENSG00000159348	CYB5R1
gene.clic	ENSG00000175197	DDIT3
gene.clic	ENSG00000168209	DDIT4
gene.clic	ENSG00000136986	DERL1
gene.clic	ENSG00000125977	EIF2S2
gene.clic	ENSG00000184110	EIF3C
gene.clic	ENSG00000187840	EIF4EBP1
gene.clic	ENSG00000221968	FADS3
gene.clic	ENSG00000135842	FAM129A
gene.clic	ENSG00000116717	GADD45A
gene.clic	ENSG00000106105	GARS
gene.clic	ENSG00000130513	GDF15
gene.clic	ENSG00000165678	GHITM
gene.clic	ENSG00000138604	GLCE
gene.clic	ENSG00000100522	GNPNAT1
gene.clic	ENSG00000120053	GOT1
gene.clic	ENSG00000166123	GPT2

gene.clic	ENSG00000172432	GTPBP2
gene.clic	ENSG00000143575	HAX1
gene.clic	ENSG00000051108	HERPUD1
gene.clic	ENSG00000100292	HMOX1
gene.clic	ENSG00000113013	HSPA9
gene.clic	ENSG00000196305	IARS
gene.clic	ENSG00000006652	IFRD1
gene.clic	ENSG00000163463	KRTCAP2
gene.clic	ENSG00000133706	LARS
gene.clic	ENSG00000104660	LEPROTL1
gene.clic	ENSG00000196365	LONP1
gene.clic	ENSG00000166986	MARS
gene.clic	ENSG00000135272	MDFIC
gene.clic	ENSG00000172167	MTBP
gene.clic	ENSG00000120254	MTHFD1L
gene.clic	ENSG00000065911	MTHFD2
gene.clic	ENSG00000134440	NARS
gene.clic	ENSG00000082641	NFE2L1

gene.clic	ENSG00000165030	NFIL3
gene.clic	ENSG00000087269	NOP14
gene.clic	ENSG00000176046	NUPR1
gene.clic	ENSG00000089723	OTUB2
gene.clic	ENSG00000163291	PAQR3
gene.clic	ENSG00000100889	PCK2
gene.clic	ENSG00000067057	PFKP
gene.clic	ENSG00000130024	PHF10
gene.clic	ENSG00000092621	PHGDH
gene.clic	ENSG00000087074	PPP1R15A
gene.clic	ENSG00000146733	PSPH
gene.clic	ENSG00000073008	PVR
gene.clic	ENSG00000183010	PYCR1
gene.clic	ENSG00000113643	RARS
gene.clic	ENSG00000144468	RHBDD1
gene.clic	ENSG00000031698	SARS
gene.clic	ENSG00000121064	SCPEP1
gene.clic	ENSG00000130766	SESN2

gene.clic	ENSG00000182199	SHMT2
gene.clic	ENSG00000181788	SIAH2
gene.clic	ENSG00000115902	SLC1A4
gene.clic	ENSG00000105281	SLC1A5
gene.clic	ENSG00000171612	SLC25A33
gene.clic	ENSG00000168003	SLC3A2
gene.clic	ENSG00000196517	SLC6A9
gene.clic	ENSG00000151012	SLC7A11
gene.clic	ENSG00000165349	SLC7A3
gene.clic	ENSG00000103257	SLC7A5
gene.clic	ENSG00000167780	SOAT2
gene.clic	ENSG00000164647	STEAP1
gene.clic	ENSG00000113407	TARS
gene.clic	ENSG00000156787	TBC1D31
gene.clic	ENSG00000187735	TCEA1
gene.clic	ENSG00000177426	TGIF1
gene.clic	ENSG00000101255	TRIB3
gene.clic	ENSG00000024048	UBR2

gene.clic	ENSG00000065060	UHRF1BP1
gene.clic	ENSG00000112715	VEGFA
gene.clic	ENSG00000184575	XPOT
gene.clic	ENSG00000134684	YARS